Third harmonic cavity design and RF measurements for the Frascati DAΦNE collider

David Alesini, Roberto Boni, Alessandro Gallo, Fabio Marcellini, and Mikhail Zobov
INFN Laboratori Nazionali di Frascati, P.O. Box 13, I-00044, Frascati (Roma), Italy

Mauro Migliorati and Luigi Palumbo
INFN Laboratori Nazionali di Frascati, P.O. Box 13, I-00044, Frascati (Roma), Italy
and Department Energetica, University "La Sapienza," Via Antonio Scarpa 14, 00161 Roma, Italy
(Received 19 December 2003; published 7 September 2004)

Third harmonic passive RF cavities have been proposed for installation in both rings of the DAΦNE factory collider to improve the Touschek lifetime and to increase the Landau damping. This paper illustrates the design of the harmonic cavities. The main requirements were to obtain a relatively low R/Q factor and a quality factor Q as high as possible to satisfy beam dynamics requirements and to damp all the higher order mode (HOM) to a harmless level in order to avoid multibunch instabilities. A spherical shape of the cavity central body has been chosen as an optimum compromise between a high Q resonator and a low R/Q factor. HOM suppression has been provided by a ferrite ring damper designed for the superconducting cavities of the high energy ring of the KEK-B factory. The design and electromagnetic properties of the resonant modes have been studied with MAFIA and HFSS codes. Cavities have been made of aluminum and the RF measurements have been performed to characterize them. The measurements are in a good agreement with numerical simulations results, demonstrating a satisfactory HOM damping.

DOI: 10.1103/PhysRevSTAB.7.092001 PACS numbers: 42.60.Da, 41.75.Lx

I. INTRODUCTION

The Frascati Φ factory DAΦNE [1] is a double ring, high luminosity collider working at the energy of the Φ-meson resonance (1.02 GeV in the center of mass). The most relevant DAΦNE parameters for luminosity delivery to the KLOE experiment (runs of year 2002) are summarized in Table I.

The installation of a third harmonic cavity in each DAΦNE ring has been proposed to increase the Touschek lifetime and to weaken the coherent instabilities by increasing the Landau damping due to the nonlinearity of the harmonic voltage [2]. The implications of the harmonic voltage on the multibunch beam dynamics have been carefully considered elsewhere [3]. The cavity

TABLE I. DAΦNE parameters (KLOE runs 2002).

Energy	E [MeV]	510
Max. beam current	I_M [A]	1.2 (presently), 1.4–1.7 (goal)
Number of colliding bunches	N_b	47–51
Max. current per bunch	I_b [mA]	25 (presently), 30–35 (goal)
RF frequency	f_{RF} [MHz]	368.29
RF voltage	V_{RF} [kV]	100–150
Revolution frequency	f_0 [MHz]	3.069
Harmonic number	h	120
Bunch spacing	T_b [ns]	5.43 ($= 2/f_{\mathrm{RF}}$)
Synchrotron losses	E_r [keV/turn]	9.3
Parasitic losses	E_p [keV/turn]	$\approx$ 2.5 (at $I_b \approx 20$ mA, e^- ring)
		$\approx$ 4.5 (at $I_b \approx 20$ mA, e^+ ring)
Momentum compaction	α_c	≈ 0.034
Natural bunch length	σ_{z0} [cm]	$\approx$ 1.6 (at $I_b \approx 0$ mA, $V_{\mathrm{RF}} \approx 120$ kV)
Nat. bunch energy spread	σ_E/E	3.9×10^{-4}
Bunch length (lengthening regime)	σ_z [cm]	$\approx$ 2.4 (e^+, at $I_b \approx 20$ mA, $V_{\mathrm{RF}} \approx 120$ kV)
		$\approx$ 2.8 (e^-, at $I_b \approx 20$ mA, $V_{\mathrm{RF}} \approx 120$ kV)
Vertical to horizontal emittance coupling	$\kappa = \varepsilon_y/\varepsilon_x$	$\approx 0.2\%$
Vertical beta function at IP	β_y^* [cm]	≈ 3
RF acceptance	$\varepsilon_{\mathrm{RF}}/E$	$\approx 0.55\%$ (at $V_{\mathrm{RF}} \approx 120$ kV
Beam lifetime	τ_T [s]	$\approx$ 1000–2000

TABLE II. DAΦNE parameter set with the harmonic system.

Main RF voltage	V_{RF} [kV]	200
Main cavity shunt impedance	$R_s = V^2/2P_{\mathrm{RF}}$ [MΩ]	1.9
Main cavity Q factor	Q_0	31 500
Main cavity input coupling factor	$\boldsymbol{\beta}$	≈ 4.6
RF harmonic frequency	f_H [MHz]	$1104.87 = 3f_{\mathrm{RF}}$
RF harmonic voltage	V_H [kV]	56
Harmonic cavity shunt impedance	$R_H = V^2/2P_H$ [MΩ]	0.48
Harmonic cavity Q factor	Q_{0_H}	18 500
Natural bunch length	σ_{z0} [cm]	≈ 2.5 (at $I_b \approx 0$ mA)
Bunch length (lengthening regime)	σ_z [cm]	≈ 3.1 (at $I_b \approx 35$ mA)
RF acceptance	$\varepsilon_{\mathrm{RF}}/E$	$\approx 0.7\%$

has been designed, built, and measured. Soon it will be installed on the collider rings. A set of DAΦNE RF parameters with the harmonic system is given in Table II.

In this paper we describe the design of the third harmonic cavity aimed at the damping of all higher order modes (HOM) and we discuss the results of numerical simulations (Sec. II) comparing them with experimental measurements (Sec. III).

Because of the peculiarity of the DAΦNE parameters (low RF voltage, high beam current), powering the cavity in the passive way appears to be the simplest and the most effective choice. The required harmonic voltage can be obtained with modest cavity shunt impedance and over a wide range of beam currents. The choice of the third harmonic of the main RF frequency has been done as a good trade-off between efficiency and compactness requirements.

The harmonic cavity has been designed to obtain a relatively low R/Q factor, preserving as much as possible the Q value and to suppress the HOMs. To obtain this the cavity cell has been designed with a spherical shape and the HOM damping has been obtained by incorporating in the cavity design the small beam pipe (SBP) ferrite load developed at KEK-B for the HER superconducting (SC) cavity [4]. The adopted HOM damping scheme is similar to that proposed for the B-Factories crab cavity [5] and is widely discussed in Sec. II. The use of the SBP ferrite ring, incorporated in the cavity structure, guarantees simultaneously (1) an effective broadband damping of the cavity HOM, (2) a widely open design of the cell which is suitable for obtaining a moderate value of the R/Q factor, and (3) a simplification of both the simulation and the manufacturing processes.

The simplicity of the geometry and the naturally associated moderate R/Q were the main reasons to prefer this design approach with respect to that of a single cell loaded with off-axis rectangular or ridged waveguides.

The harmonic voltage can be almost completely "switched off" by tuning the cavity as far as possible from the harmonic $3h$. In order to minimize the coherent effects [3], it is worth tuning the cavity at $3h + (n + 1/2)f_{\mathrm{rev}}$ (f_{rev} is the revolution frequency) with the integer n as high as the tuning system allows. This is the so-called "parking option" that can be used to recover approximately the usual operating conditions established before the harmonic cavity installation. In this case, as predicted by simulations, a nonzero longitudinal and transverse impedance of a quadrupole mode perturbed by the plunger insertion has been found by measurements, as discussed in Sec. III.

II. HARMONIC CAVITY DESIGN

The design of the harmonic cavity has been aimed to obtain a relatively low R/Q factor, preserving as much as possible the Q value for beam dynamics considerations discussed in [3], and to suppress the HOM. The final designed shape is shown in Fig. 1, where (a) a spherical shape of the cell has been adopted as an optimum compromise between a high Q resonator and a moderate R/Q factor and (b) HOM damping has been obtained by incorporating in the cavity design the SBP ferrite load developed at KEK-B for the HER SC cavity [4] and adopting an HOM damping scheme similar to that proposed for the B-Factories crab cavity [5].

The ferrite load is coupled with the HOM and completely decoupled with respect to the field of the accelerating mode. A coaxial cylinder shields the ferrite load preventing direct exposure to the circulating beam charge.

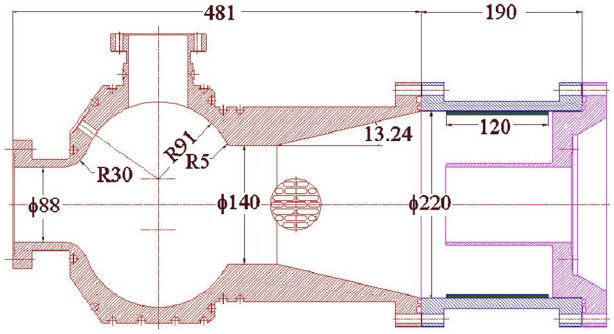

FIG. 1. (Color) Sketch of the DAΦNE third harmonic cavity.

The use of the SBP ferrite ring of the KEK-B HER SC cavity guarantees an effective broadband damping of the cavity HOM, and its reliability under high-current operating conditions has been experimentally proven at KEK-B. Moreover, the incorporation of such a load in the cavity structure leads to a widely open design of the cell, which is also suitable for obtaining a moderate value of the R/Q factor. The resulting assembly preserves a basic azimuthal symmetry, which drastically simplifies both the simulation and the manufacturing processes. The simplicity of the geometry and the naturally associated moderate R/Q were the main reasons to prefer this design approach with respect to that of a single cell loaded with off-axis rectangular or ridged waveguides, which is more indicated whenever the optimization of the cavity efficiency is essential.

Besides, the ferrite load shielding through the insertion of an internal cylinder is a conservative approach to keep the cavity contribution to the machine broadband impedance under control. In particular, it has been calculated that the shielded cavity gives a small contribution to the overall DAΦNE wakefield [6]. The numerical tracking of the intrabeam particle motion taking into account this additional harmonic cavity contribution has not revealed any noticeable changes in the single bunch dynamics. In the case of unshielded ferrite, it is not obvious how to make a similar estimate since the direct interaction between the beam and the ferrite ring needs to be modeled up to frequencies of about 20 GHz.[1] Moreover, we could not rely on the single bunch dynamics experimental results obtained at KEK-B HER, being the DAΦNE energy is much lower and the bunch current much larger. Finally, according to our budgetary evaluation, the shield also reduces the power dissipated on the HOM load since it eliminates the contribution coming from the direct exposure of the ferrite to the beam. Details of power dissipation distribution and cavity cooling system, together with other engineering aspects, are reported elsewhere [7].

A large port on the rounded cell top for the insertion of a tuning plunger and one of the three small ports for housing the RF probes to measure the beam-induced field are also visible in Fig. 1.

A. 2D simulation results

The cavity modes have been calculated by means of the MAFIA [8] and HFSS [9] codes in order to define the dimensions of the cavity. The simulated 2D profile is reported in Fig. 2. The simulations were aimed to obtain simultaneously (a) R/Q of the fundamental mode of about 25 Ω with a Q as high as possible, (b) a strong coupling of the cavity HOM with the damper and a weak coupling with the fundamental one, and (c) limited dimensions of the cavity because of the mechanical constraints for the structure allocation in the ring.

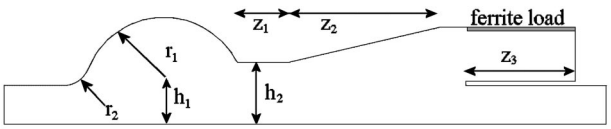

FIG. 2. Cavity profile simulated by MAFIA and HFSS.

For this purpose the radii r_1 and r_2 of the rounded cell and the dimensions h_1, h_2, z_1, and z_2 (Fig. 2) have been properly tuned. Furthermore, to reduce the cost it has been decided to build the cavity body in aluminum instead of copper even if this implies a reduction of the fundamental mode Q factor by ~20%.

Since the electromagnetic (e.m.) properties of the special ferrite used in the HOM dampers vary with the frequency [10], in the simulations we considered the average permittivity and permeability complex values over the frequency span of interest.

The resonant frequencies (f), the R/Q, and the Q values of the cavity longitudinal modes (M: monopole) as given by the MAFIA simulations of the 2D profile are reported in Table III (the HFSS simulations give substantially the same results).

The resonant frequencies and the transverse impedances for the dipole modes (D) are reported in Table IV while in Table V the frequencies and the Q factors of the quadrupole (Q), sextupole (S), and octupole (O) modes are listed.

Some of these modes are weakly coupled with the damper (high Q factors) but they do not have, for particles traveling near the cavity axis, significant longitudinal and transverse impedances [11].

The beam pipe cutoff frequency of the TM_{01} longitudinal mode is about 2.6 GHz, while that of the TE_{11} transverse mode is about 2 GHz. We limited our simulations of longitudinal and transverse modes to these cutoff frequencies since above them the modes are supposed to be damped by propagating all along the vacuum pipe. Moreover, the beam spectrum and the coupled-bunch instability form factor rolls off at about 2–2.5 GHz for typical values of the DAΦNE bunch length.

The magnitude of the electric field of the working mode M_1 and of the HOM M_4 are plotted in Fig. 3, as obtained by HFSS. In the M_1 mode case the e.m. field vanishes in the tapered transition and only a negligible amount of power can reach the damper while in the M_4 mode case the e.m. field propagates through the transition toward the ferrite load.

HFSS simulations exciting the cavity by two RF probes have also been performed. The obtained R and Q values

[1]Standard codes for calculating wakefield in time domain (like MAFIA) do not treat materials with complex and/or frequency dependent values of the dielectric constant and permittivity (as the case of the ferrites).

TABLE III. Longitudinal modes obtained by measurements and compared with the simulations in the case of tuned cavity.

	MAFIA simulations			Measurements		
	f	Q	R/Q [Ω]	f [GHz]	Q	R/Q [Ω]
M_1	1.105	23 000	26	1.105	18 500	21.4
M_2	1.335	10	16	not measurable (n.m.)	n.m.	n.m.
M_3	1.600	30	6	n.m.	n.m.	n.m.
M_4	1.650	50	2	1.65	168	16.8
M_5	1.899	50	4	n.m.	n.m.	n.m.
M_6	2.094	110	7	2.100	224	n.m.
M_7	2.270	120	9	2289	60	n.m.
M_8	2.495	170	3	2.466	140	n.m.
M_9	2.524	230	10	2.507	278	n.m.

TABLE IV. Transverse modes obtained by measurements and compared with the simulations in the case of tuned cavity.

	MAFIA simulations			Measurements		
	F	Q	R_T/Q [Ω/m]	f [GHz]	Q	R/Q [Ω/m]
D_1	1.089	438	66	1.070	450	146
D_2	1.244	35	26	n.m.	n.m.	n.m.
D_3	1445	158	22	1.400	139	29
D_4	1.618	158	29	1.560	175	n.m.
D_5	1.797	266	37	1.725	163	n.m.
D_6	1.886	283	24	1.865	190	74

confirm the previous simulation results and the resulting $|S_{12}|$, for the longitudinal and dipole modes, is shown in Fig. 4.

B. 3D simulation results

The tuner inserted in the cavity allows controlling the resonant frequency of the cavity accelerating mode to regulate the harmonic voltage or to "park" the cavity itself.

Since it perturbs the 2D profile of the structure, two relevant effects have been examined.

TABLE V. Quadrupole (Q), sextupole (S), and octupole (O) cavity modes obtained by 2D MAFIA simulations.

	f [GHz]	Q
Q_1	1.597	19 700
Q_2	1.975	340
Q_3	2.078	30
Q_4	2.242	40
Q_5	2.323	40
Q_6	2.398	90
Q_7	2.448	130
S_1	2.042	36 930
S_2	2.469	12 400
O_1	2.471	36 700

(a) The degradation of the Q factor of the fundamental mode caused by the strong field in the gap between the tuner plunger and its surrounding cylinder. According to our numerical simulations, the expected reduction of the Q value with respect to 2D results is ~20% with the cavity properly tuned and ~30% with the tuner in the parking option position. The magnitude of the H field between the tuner and the outer cylinder for the fundamental mode as obtained by MAFIA is plotted in Fig. 5.

(b) The appearance, in the case of "parked cavity," of longitudinal and transverse impedance due to the quadrupole mode Q_1. In fact, while in the 2D symmetric geometries the quadrupole mode does not contribute to the transverse and longitudinal impedance (for particles

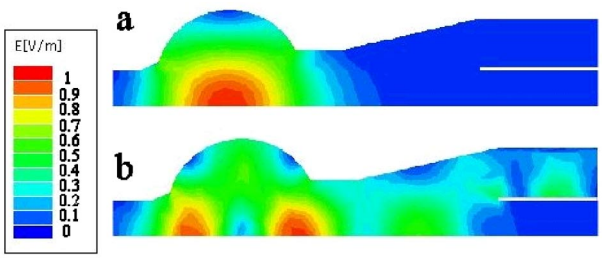

FIG. 3. (Color) Magnitude of the electric field of the working mode M_1 (a) and of the HOM M_4 (b) obtained by HFSS.

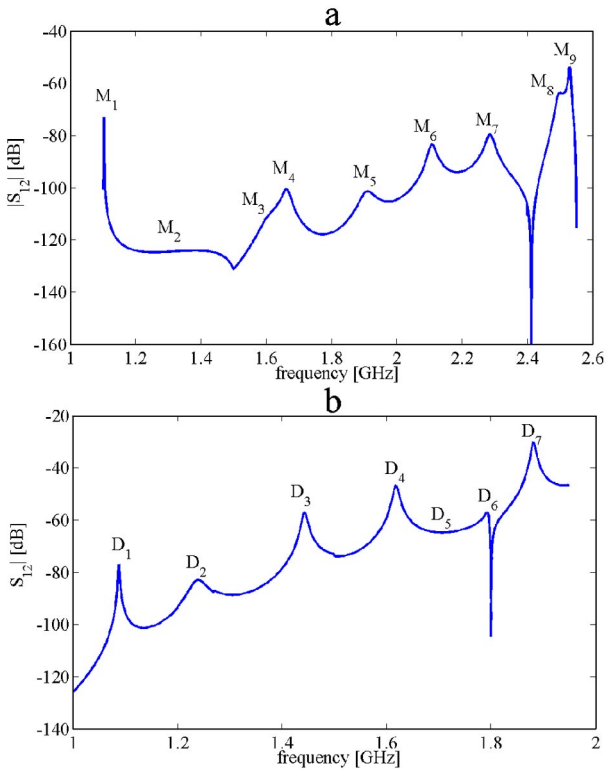

FIG. 4. (Color) $|S_{12}|$ obtained by HFSS exciting the longitudinal (a) and dipole (b) modes by two RF probes.

traveling on axis), in this case, the presence of the tuner strongly perturbs the symmetry of the cavity inducing a nonzero longitudinal and transverse impedance (on axis). In Fig. 6 the longitudinal electric field of this quadrupole mode with the tuner deeply inserted as obtained by HFSS is plotted. When the tuner is inserted to shift the fundamental mode at 1.113 GHz ($\cong 3f_{\mathrm{RF}} + 2.5f_0$), HFSS provides for this mode: $f \cong 1.559$ GHz, $Q \cong 10\,000$, $R/Q \cong 0.59\ \Omega$, and $R_T/Q \cong 0.1\ \Omega/\mathrm{m}$.

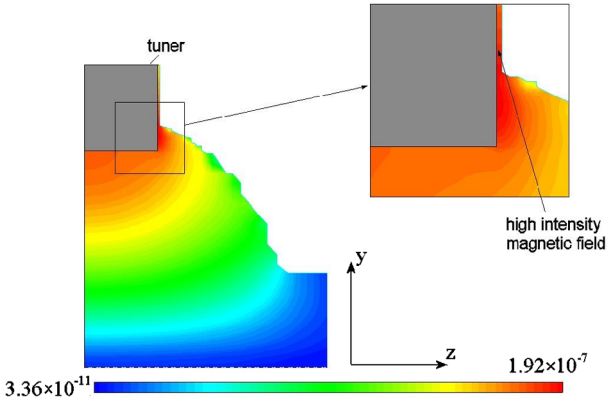

FIG. 5. (Color) Magnitude of the B field between the tuner and the outer cylinder corresponding to the fundamental mode as obtained by MAFIA 3D simulation.

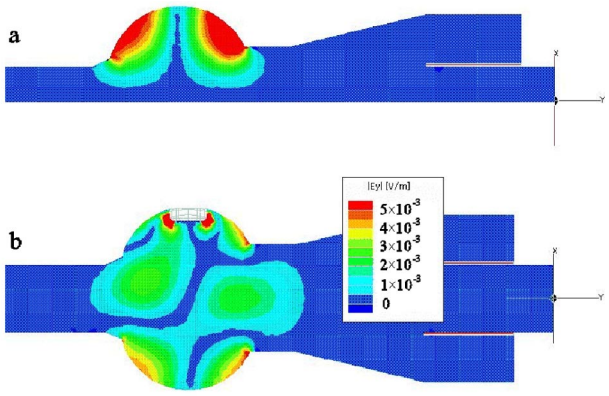

FIG. 6. (Color) Electric field of the quadrupole mode Q_1 obtained by HFSS without the tuner (a) and with the tuner deeply inserted (b).

III. MEASUREMENT RESULTS

The picture of the DAΦNE harmonic cavity is shown in Fig. 7.

The RF measurements of the following two types have been carried out: (a) measurement of port-to-port transmission coefficient ($|S_{12}|$) between two probes to find the resonant frequencies and the Q factors of the fundamental and HOM; (b) wire measurements necessary to evaluate both the longitudinal and vertical coupling impedance. As discussed in [12], this method allows measuring the impedances with good precision in the case of "lumped impedances" despite the fact that the wire perturbs both the field configuration and the resonant frequencies of the cavity modes. In our case both the longitudinal and vertical impedances are not properly "lumped" elements and, furthermore, the wire itself modifies the HOM coupling with the damper ring, as we will discuss below. However, this kind of measurement can give some useful information on the impedance content of the cavity.

We did not perform perturbative bead-pull measurements, since from our experience they are not suitable to

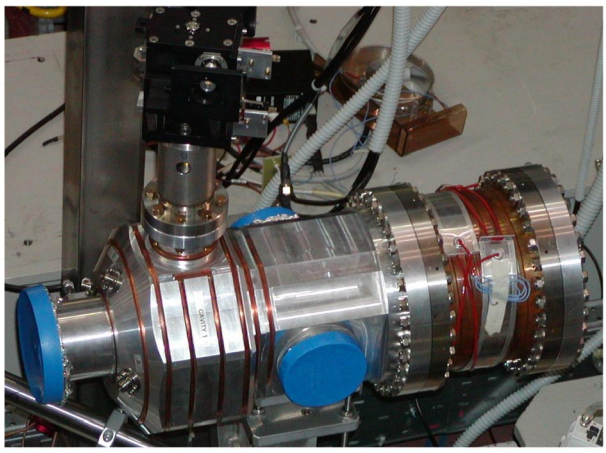

FIG. 7. (Color) Picture of the DAΦNE harmonic cavity.

characterize heavily damped modes. In this case, due to the resulting low Q values, the modes mix together and it is difficult to select and isolate a single mode in a port-to-port measurement. Moreover, the frequency shift induced by the perturbating object is a very small fraction of the damped mode bandwidth, spoiling the quality of the measurement.

A. Tuned cavity

The resonant frequencies f, the R/Q's, and the Q values of the cavity longitudinal (M) and transverse (D) modes are reported in Tables III and IV.

The modes have been measured in the case of tuned cavity and compared with the simulations of the 2D MAFIA structure. The resonant frequencies (f) and the Q values of the modes have been calculated by fitting the port-to-port transmission coefficient (reported in Fig. 8) between two RF probes while the R/Q's have been obtained by the wire measurement (reported in Figs. 9 and 10). As well predicted by simulations, the ferrite load damps all the longitudinal and transverse modes with the exception of the fundamental one (M_1).

Some modes, calculated by simulations, are not measurable on the prototype because of the low Q values and because of the presence of higher polarity modes with high Q factors (quadrupoles, sextupoles, octupoles) located in the same frequency band.

As observed before, the results obtained by the wire measurement have to be carefully analyzed. In fact, the wire itself perturbs both the resonant frequency of the modes and also their field configuration, as can be seen in HFSS simulations of the cavity + wire system. The coupling with the ferrite damper can be strongly affected. For example, the field resulting from a HFSS simulation of the monopole M_4 wire measurement is shown in Fig. 11.

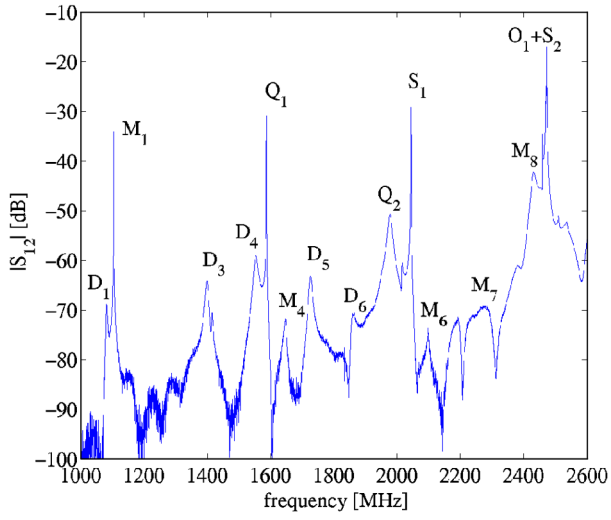

FIG. 8. (Color) $|S_{12}|$ between two RF probes in the case of tuned cavity.

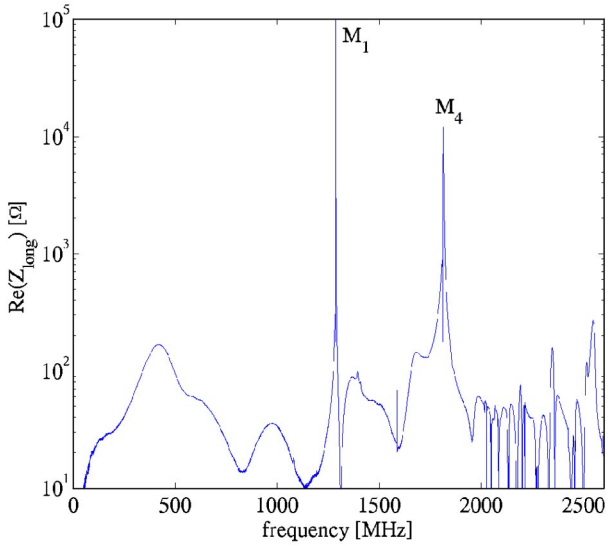

FIG. 9. (Color) Longitudinal impedance obtained by wire measurement method in the case of tuned cavity.

Without the wire [Fig. 11(a)] the mode propagates along the tapered transition toward the ferrite load. Instead, with the wire [Fig. 11(b)] the e.m. field preferably propagates along the internal coaxial line formed by the wire and the beam pipe, and the ferrite load is bypassed. Consequently, the mode is no more damped and a high impedance value is measured at ~1.8 GHz, as shown in Fig. 9.

Assuming a bunch length larger than 2.5 cm, the longitudinal and transverse HOM's effective impedances are lower than 800 Ω and 25 kΩ/m, respectively.

These contributions will not change significantly the present scenario of the DAΦNE coupled-bunch dynamics while, to the contrary, beneficial contributions are expected from the Landau damping associated to the large nonlinearity of the harmonic voltage.

The resonant frequency of the fundamental mode as a function of the tuner position is shown in Fig. 12. As predicted by the HFSS simulations the cavity can be tuned in the $3f_{RF} - 1.5f_0$ to $3f_{RF} + 3.5f_0$ range which is wide enough to operate the cavity at various currents or to park it away from the beam harmonic $3h$.

In Fig. 13 the coupling coefficient (β) of the three probes and the corresponding external Q factor (Q_{EXT}) is shown, as a function of the resonant frequency of the cavity. Probes 1 and 3 are symmetric with respect to the tuner (both in the horizontal plane) and their β factors (or Q_{EXT}) show the same dependence on the tuner position. Probe 2 is placed in the vertical plane and the perturbation of the local fields due to the tuner penetration is different with respect to that of probes 1 and 3.

B. Parked cavity

A full characterization of the cavity has been performed also when the tuner is in the parking position

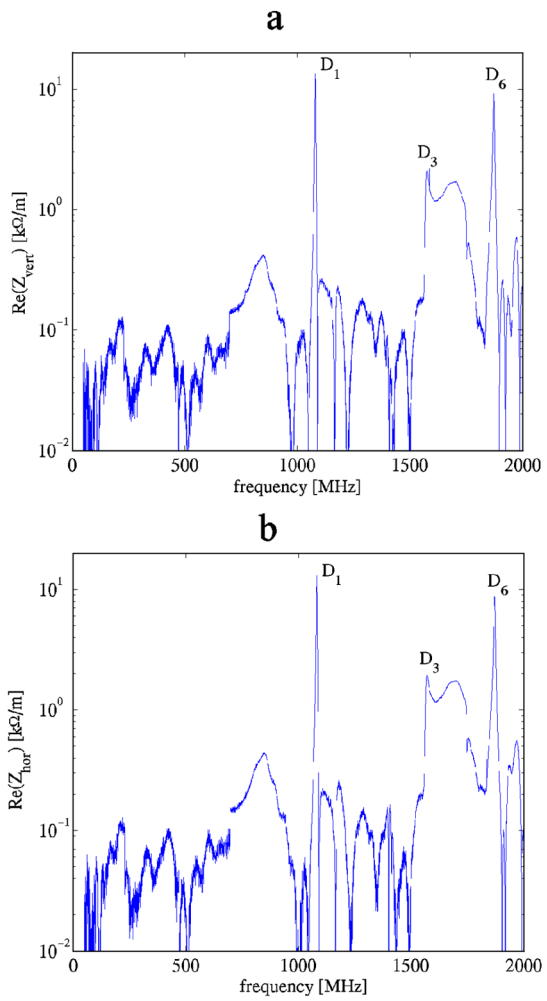

FIG. 10. (Color) Vertical (a) and horizontal (b) impedances obtained by the wire measurement method in the case of tuned cavity.

$f_{\mathrm{HCAV}} = 3f_{\mathrm{RF}} + 2.5f_0$. In this case, as predicted by simulations, nonzero longitudinal and transverse impedance for the quadrupole mode Q_1 has been found. As an example, the longitudinal spectrum of the parked cavity measured with the wire technique is reported in Fig. 14. A sizable monopole component coming from the plunger perturbed quadrupole is visible. While parking the cavity

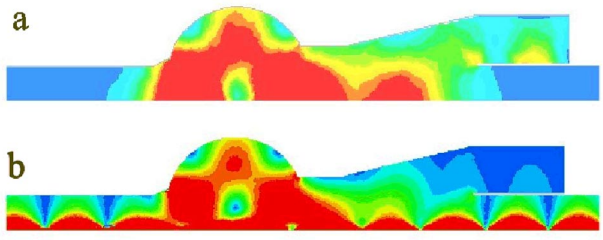

FIG. 11. (Color) Electric field configuration of the mode M4 obtained by HFSS simulation: (a) without the wire (b) with the wire.

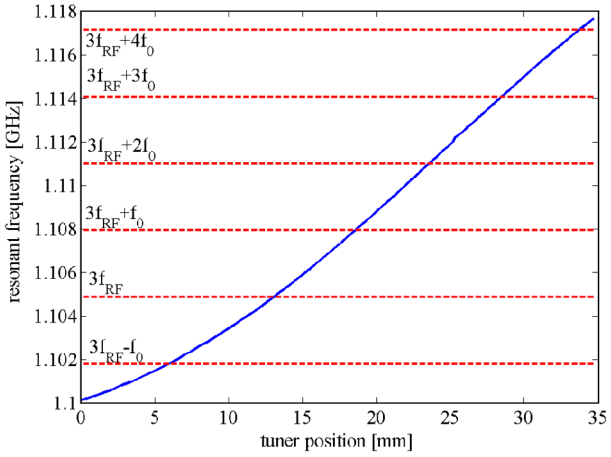

FIG. 12. (Color) Measured resonant frequency of the fundamental mode as a function of the tuner position.

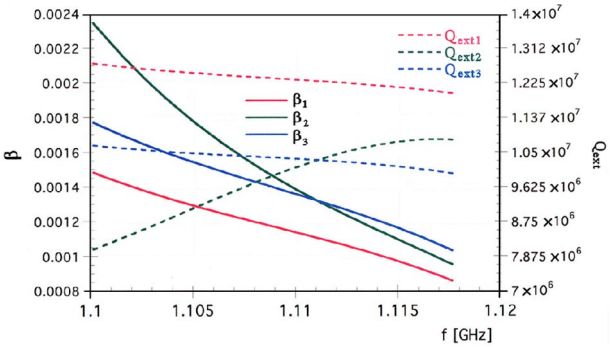

FIG. 13. (Color) Measured coupling coefficient β and external Q factors for the three probes as a function of the resonant frequency.

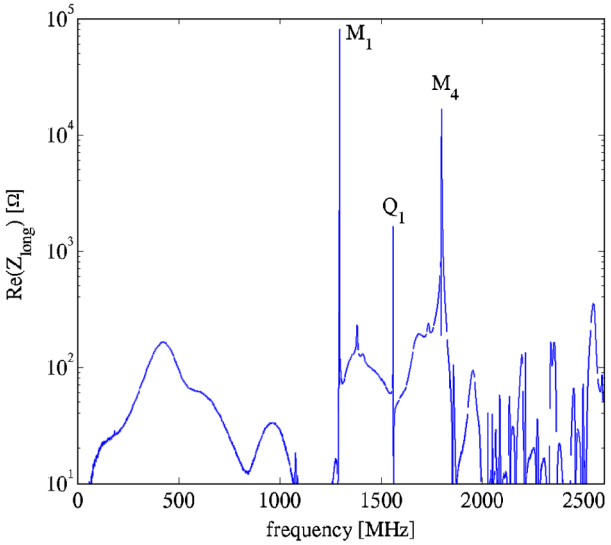

FIG. 14. (Color) Longitudinal impedance obtained by the wire measurement method in the case of parked cavity.

it is also worth checking the frequency position of this mode to limit the coupling with beam unstable sidebands.

As a general conclusion, looking at the effective impedance values, it is reasonable to assume that the present scenario of DAΦNE beam dynamics will not be significantly changed even in the parked cavity case.

IV. CONCLUSIONS

In this paper we have described the design of the DAΦNE passive third harmonic cavity. The main design requirements were (a) to obtain a relatively low R/Q factor and a quality factor Q as high as possible to satisfy beam dynamics requirements; (b) to damp all the HOMs to a harmless level in order to avoid multibunch instabilities and high power RF losses; (c) to provide a cavity structure compact enough to fit the limited available space for the allocation in the ring.

The HOM damping has been achieved by adopting a scheme similar to that proposed for the B-Factories crab cavity. In that scheme the HOM e.m. field is dissipated in a ferrite ring damper, the same as used in the KEK-B SC cavities of HER, and provided by the KEK Laboratory.

The design and e.m. properties of the resonant modes have been studied with MAFIA and HFSS e.m. codes.

Both transverse and longitudinal coupling impedances of the cavity have been measured by coaxial wire methods.

The simulation results and measurements made on the cavity are in agreement. In particular, they have shown that (a) all the HOMs in the cavity are well damped so that they will not change significantly the present scenario of the DAΦNE beam dynamics from the point of view of single and multibunch instabilities and (b) the R/Q factor of the fundamental mode is about 25 Ω with a Q of about 20 000. These are suitable values to operate the cavity in the passive mode.

ACKNOWLEDGMENTS

We thank Dr. Takaaki Furuya and the KEK Laboratory for supplying us three SBP dampers giving us all the information necessary to put them in operation. We would like to acknowledge A. Clozza for the vacuum tests and conditioning of the ferrite dampers. Thanks also to G. Fontana and V. Lollo for the technical support and to P. Baldini, S. Quaglia, and M. Scampati for their support during the RF measurements.

[1] M. Zobov, D. Alesini, G. Benedetti, S. Bertolucci, M. E. Biagini, C. Biscari, R. Boni, M. Boscolo, A. Clozza, G. Delle Monache, G. Di Pirro, A. Drago, A. Gallo, A. Ghigo, S. Guiducci, M. Incurvati, C. Ligi, F. Marcellini, G. Mazzitelli, C. Milardi, L. Pellegrino, M. A. Preger, P. Raimondi, R. Ricci, C. Sanelli, F. Sannibale, M. Serio, F. Sgamma, A. Stecchi, A. Stella, C. Vaccarezza, and M. Vescovi, in *Proceedings of the 2002 European Particle Accelerator Conference, Paris* (EPS-IGA/CERN, Geneva, 2002), p. 443.

[2] M Migliorati, L. Palumbo, and M. Zobov, Nucl. Instrum. Methods Phys. Res., Sect. A **354**, 215 (1995).

[3] D. Alesini, A. Gallo, S. Guiducci, F. Marcellini, M. Migliorati, L. Palumbo, and M. Zobov, Phys. Rev. ST Accel. Beams **6**, 074401 (2003).

[4] T. Tajima, KEK Report No. 2000-10, 2000.

[5] K. Akai, J. Kirchgessner, D. Moffat, H. Padamsee, J. Sears, T. Stowe, and M Tigner, in *Proceedings of B Factories The State of the Art in Accelerators, Detectors and Physics, 1992* (SLAC, Stanford, CA, 1992), p. 181.

[6] M. Zobov, A. Drago, A. Gallo, A. Ghigo, F. Marcellini, M. Migliorati, L. Palumbo, M. Serio, and G. Vignola, Physics/0312072.

[7] L. Pellegrino, DAΦNE Technical Note No. ME-14, INFN-LNF, 2003 (in Italian).

[8] www.cts.de

[9] www.ansoft.com

[10] W. Hartung, D. Moffat, T. Hays, K. Akai, Ph. Barnes, J. Kirchgessner, D. Metzger, H. Padamsee, D. Rubin, J. Sears, and V. Veshcherevich, in *Proceedings of the Workshop on Microwave-Absorbing Materials for Accelerators, Newport News, VA, 1993* (Jefferson Laboratory, Newport News, VA, 1993), p. 162.

[11] L. Palumbo, V. Vaccaro, and M. Zobov, CERN Report No. 95-06, 1995, Vol. 1.

[12] H. Hahn and F. Pedersen, BNL Report No. BNL 50870, 1978.